

NeSt-VR: An Adaptive Bitrate Algorithm for Virtual Reality Streaming over Wi-Fi

Miguel Casanovas^{*1}, Ferran Maura^{*1}, Ishtar Vandebroek², Haryo Sukmawanto², Eric Joris², and Boris Bellalta¹

¹Universitat Pompeu Fabra, Barcelona, Spain

Email: {firstname.lastname}@upf.edu

²CREW, Brussels, Belgium

Email: lab@crew.brussels

Abstract—Real-time interactive Virtual Reality (VR) streaming is a significantly challenging use case for Wi-Fi given its high throughput and low latency requirements, especially considering the constraints imposed by the possible presence of other users and the variability of the available bandwidth. Adaptive BitRate (ABR) algorithms dynamically adjust the encoded bitrate in response to varying network conditions to maintain smooth video playback. In this paper, we present the *Network-aware Step-wise ABR algorithm for VR streaming* (NeSt-VR), a configurable algorithm implemented in Air Light VR (ALVR), an open-source VR streaming solution. NeSt-VR effectively adjusts video bitrate based on real-time network metrics, such as frame delivery rate, network latency, and estimated available bandwidth, to guarantee user satisfaction. These metrics are part of a comprehensive set we integrated into ALVR to characterize network performance and support the decision-making process of any ABR algorithm, validated through extensive emulated experiments. NeSt-VR is evaluated in both single- and multi-user scenarios, including tests with network capacity fluctuations, user mobility, and co-channel interference. Our results demonstrate that NeSt-VR successfully manages Wi-Fi capacity fluctuations and enhances interactive VR streaming performance in both controlled experiments at UPF’s lab and professional tests at CREW’s facilities.

Index Terms—Virtual Reality, Video Streaming, Adaptive Bitrate, Wi-Fi, ALVR, Experimental Evaluation

I. INTRODUCTION

Virtual, Mixed, and Augmented Reality (VR, MR, AR), technologies encompassed by the term eXtended Reality (XR), have increased in popularity over the last decade [1], driven by the widespread availability of consumer XR Head-Mounted Displays (HMDs) such as the HTC Vive, Valve Index, and Meta Quest. Since *local rendering* (performing rendering directly on the user’s device) is limited by the device’s computational capabilities, *remote rendering* [2] (offloading the computational workload to powerful cloud or edge computing servers) is often required, particularly for applications with high graphical demands.

Traditionally, remote rendering has relied on wired connections to ensure low-latency, high-bandwidth transmissions. However, wireless technologies such as 5G and Wi-Fi provide greater flexibility, especially for mobile XR applications, as they enable users to move freely without being tethered to a physical connection [3]. Among these, Wi-Fi is expected

to become the most prevalent technology for XR streaming due to its widespread adoption in home and office spaces and the anticipated improvements in throughput, reliability, and latency in future IEEE 802.11 standard revisions [4], [5].

However, Wi-Fi networks operate in unlicensed frequency bands and are susceptible to external perturbations such as co-channel interference (overlapping transmissions on the same frequency band) [6], and path loss (signal degradation due to distance from the access point or obstructions) [7]. In addition, Wi-Fi is prone to channel contention (competition for access to the wireless medium) and network congestion (demand exceeding available bandwidth), particularly in high-density environments [8]. These factors can cause increased latency, jitter, and packet loss, leading to visual artifacts, stuttering, and frame drops that degrade the user’s Quality of Experience (QoE) in the particular case of VR streaming [9].

To dynamically manage sporadic congestion episodes that could otherwise disrupt VR streaming sessions, Adaptive Bitrate (ABR) solutions can be employed (e.g., FESTIVE [10], BOLA [11], Google’s Congestion Control [12], and EVer-Est [13], [14]). ABR algorithms continuously adjust the video encoding bitrate based on real-time network conditions, reducing traffic load to mitigate congestion effects. This approach helps minimize stuttering, visual artifacts, black borders, and frame drops, albeit at the cost of reduced visual quality.

In this paper, we present the *Network-aware Step-wise ABR algorithm for VR streaming* (NeSt-VR). This algorithm is implemented in Air Light VR (ALVR)¹, an open-source VR streaming solution, which we have extended with a diverse set of performance metrics to provide a detailed characterization of the network state and facilitate more informed bitrate adjustments. NeSt-VR leverages several of these metrics in its decision-making process, demonstrating their effectiveness. The algorithm has been tested in both single- and multi-user scenarios, addressing network capacity fluctuations, user mobility, and co-channel interference. In particular, the contributions of this paper are:

- 1) Extending ALVR’s source code with *i*) a mechanism to receive timely feedback from the HMD at the server upon reception of a video frame (VF), and *ii*) a new set of performance metrics to characterize the network

^{*}Equal contribution

¹<https://github.com/alvr-org/ALVR>

state. The precision of these application-layer metrics has been validated by comparing them against their measured counterparts derived from Wireshark traffic traces—which include packet-related data from lower OSI layers—through multiple controlled tests emulating network impairments.

- 2) Proposing the Network-aware Step-wise ABR algorithm for VR (NeSt-VR), designed to respond effectively to sporadic Wi-Fi congestion episodes and capacity changes using several of our implemented metrics.
- 3) Highlighting the operational differences between NeSt-VR and ALVR’s native ABR solution (hereinafter referred to as *Adaptive*). Unlike *Adaptive*, which relies solely on delay-based adaptation, NeSt-VR also incorporates reliability metrics, ensuring a full Quality of Service (QoS)-aware adaptation.
- 4) Evaluating NeSt-VR’s performance in single-user and multi-user scenarios, showcasing its effectiveness in mitigating common Wi-Fi challenges, including MCS reduction due to mobility, OBSS interference, and resource contention among multiple VR users.
- 5) Evaluating NeSt-VR in the facilities of CREW, an XR company developing immersive performances, validating NeSt-VR successful operation in professional, out-of-the-lab environments.

This work extends our previous study [15] by incorporating a detailed mathematical formulation of the network performance metrics integrated into ALVR; an enhanced presentation of NeSt-VR for greater clarity and completeness, now including parameter recommendations based on user satisfaction thresholds and NeSt-VR profiles; a broader performance evaluation of NeSt-VR, incorporating multi-user and inter-network Overlapping Basic Service Set (OBSS) interference scenarios in both experimental and practical environments; and a comprehensive discussion on ABR algorithms tailored for VR streaming, addressing considerations such as objective video quality assessment and fairness in bitrate allocation.

Our fork of ALVR v20.6.0, which incorporates NeSt-VR and our extensions to ALVR, is publicly available on GitHub².

II. AIR LIGHT VR (ALVR)

A. Overview

ALVR is an open-source project that interfaces SteamVR³ to enable wireless streaming of VR content from a server to an untethered standalone HMD—such as the Meta Quest 2—over Wi-Fi. As depicted in Fig. 1, the server—acting as the streamer—sends video, audio, control data, and haptic feedback in the downlink (DL) to the HMD. On the other hand, the HMD—functioning as the client—transmits tracking, control, and statistical data in the uplink (UL) to the server.

In particular, the client gathers tracking data from its sensors and controllers, sending it to the server. On the server, this data is fed into SteamVR for pose prediction, the VR game logic is executed, and the graphical layers are rendered.

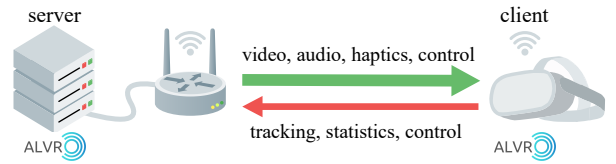


Fig. 1: ALVR streaming process.

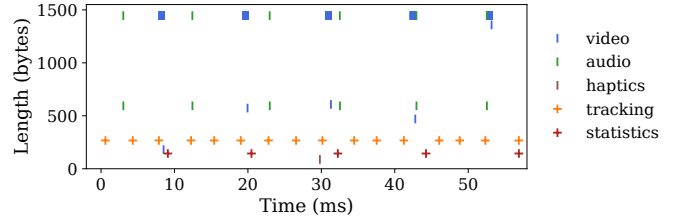


Fig. 2: ALVR v20.6.0 traffic using CBR at 100 Mbps, 90 fps, UDP, and SteamVR Home. Derived from parsed Wireshark traffic traces. Packet length includes transport headers.

These layers are combined into a VF that is encoded and fragmented into multiple packets⁴ that are sent to the client. Upon reception, the client reassembles, decodes, and processes the VF, submitting it to the VR runtime for rendering and display. At that moment, the client also sends statistical data associated with the VF to the server for logging.

As illustrated in Fig. 2, in the DL, VFs are transmitted in single bursts every $1/\text{fps}$ (i.e., every 11 ms at 90 fps) and audio data is transmitted every 10 ms, both including 1446-byte packets⁵ and a remainder of variable size. Conversely, haptic feedback is sent occasionally using 88-byte packets, depending on user actions and application-specific events. On the other hand, in the UL, tracking data is transmitted at a frequency of three updates per frame using 207-byte packets, while statistical data is sent once—upon submission of a VF to the VR runtime—using a 144-byte packet. Note that the aforementioned packet sizes include transport headers.

B. ABR algorithm

ALVR implements both Constant BitRate (CBR) and ABR for video transmission. CBR is commonly used in VR streaming to ensure consistent visual quality, as perceptible shifts in image quality may compromise the user’s sense of presence and immersion. In contrast, ABRs dynamically adjust the bitrate based on network conditions, optimizing transmission efficiency while balancing visual quality and overall performance.

ALVR’s ABR algorithm, *Adaptive*, dynamically adjusts the encoder’s target bitrate once per second. At each adjustment step, it uses the moving average of ALVR’s capacity estimate (C_{ALVR}) as the initial bitrate, then scaled by a configurable

⁴Each packet carries an application-specific prefix that includes: the payload size of the associated frame in bytes ($L_{v,f} \cdot 8$), an stream identifier, the frame index, the number of packets composing the frame (N_f), and the packet index within the frame (f)

⁵The maximum packet payload size in ALVR is configurable and defaults to 1400 bytes

²https://github.com/wn-upf/NeSt-VR/tree/extension_changes

³<https://store.steampowered.com/app/250820/SteamVR>

multiplier (default 0.9) to ensure the stream’s bitrate remains under the network’s capacity. Note that $C_{ALVR} = \frac{L_{v_f}}{d_{ntw,f}}$, where L_{v_f} represents the payload size of a VF f and $d_{ntw,f}$ denotes the network delay⁶ associated with the VF transmission.

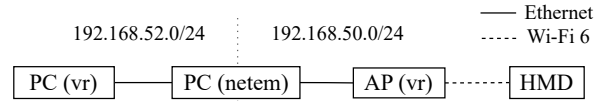
This initial bitrate is then constrained —within the configured maximum and minimum bitrate limits— in response to excessive encoder, decoder, and network delays, surpassing configurable static thresholds: $0.9 \cdot (1/\text{fps}_{target})$ ms, 30 ms, and 8 ms by default, respectively, where fps_{target} denotes the targeted frame rate. In particular, these upper limits are imposed based on the latencies deviation from their thresholds, scaling the initial bitrate proportionally.

III. EXPERIMENTAL SETUP

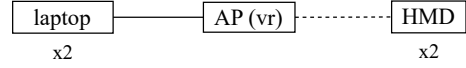
A. Equipment

Our tests in Sections IV-B, V, and VI are conducted in a controlled environment at the UPF’s Department of Information and Communication Technologies (DTIC) in Barcelona, Spain. Depending on the specific test, one of the following three setups is used: the single-user single-AP setup (Sections IV-B, V, VI-A, and VI-B), the multi-user single-AP setup (Section VI-C), and the single-user multi-AP setup (Section VI-D), as illustrated in Figs. 3a, 3b, and 3c, respectively. Equipment details can be found in Tbl. I. For VR streaming, each setup includes a gaming-centric Wi-Fi access point (AP), along with a server —functioning as the streamer— and a Meta Quest 2 HMD —acting as the client— for each user, both executing the binaries from our ALVR v20.6.0 fork. Specifically, single-user tests (setup (a) and (c)) employ a high-performance VR-ready Personal Computer (PC) as the server, while multi-user tests (setup (b)) utilize two VR-ready laptops. Setup (a) also incorporates a basic PC —placed between the server and the AP— that acts as a network emulator (netem) and uses Linux’s traffic control (tc)⁷ to emulate several network conditions such as packet loss, jitter, and limited bandwidth in the DL. On the other hand, setup (c) includes a second Wi-Fi AP for background UDP traffic delivery in the DL using *iperf3*⁸, where one laptop acts as the server and the other as the client. As illustrated in Fig. 3, the servers, netem, and APs are interconnected via 1 Gbps Ethernet cables. In contrast, clients connect wirelessly to their respective APs using Wi-Fi 6 at 5 GHz with multi-user features disabled (i.e., no OFDMA nor MU-MIMO). In setups (a) and (b), the AP operates on an 80 MHz channel bandwidth (primary channel 52), while in setup (c), both APs operate on either an 80 MHz channel bandwidth (primary channel 52) or a 40 MHz channel bandwidth (primary channel 52), resulting in fully overlapping frequency bands.

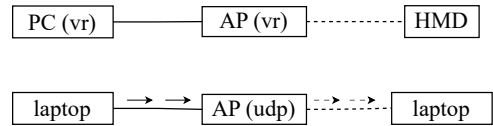
On the other hand, Section VII tests are conducted at CREW’s facilities in Brussels, Belgium. As shown in Fig. 4, the VR streaming setup includes one or two server-client



(a) Single-user, Single-AP setup.



(b) Multi-user, Single-AP setup.



(c) Single-user, Multi-AP setup.

Fig. 3: Network topologies of UPF’s lab testbed.

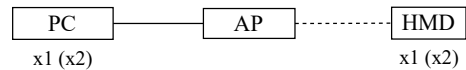


Fig. 4: Single-user (and multi-user) setup in CREW’s facilities.

pairs for single-user or multi-user tests, respectively. High-performance PCs function as servers, connected via Ethernet to an AP. The AP operates on either Wi-Fi 6 (5 GHz, primary channel 36) or Wi-Fi 6e (6 GHz, primary channel 37) at 80 MHz, with no multi-user features (i.e., no OFDMA nor MU-MIMO). HTC Vive Focus 3 HMDs serve as clients, wirelessly connected to the AP. Equipment details are provided in Tbl. II.

B. Methodology

Section IV-B and V tests are conducted without an adaptive bitrate algorithm, using a CBR of 100 Mbps. On the other hand, Section VI-A compares distinct bitrate management approaches, including CBR (100 Mbps), *Adaptive* (10 to 100 Mbps), and NeSt-VR with the *Balanced* profile (10 to 100 Mbps, init: 100 Mbps⁹). Sections VI-B, VI-C, and VI-D use CBR (100 Mbps) and NeSt-VR’s *Balanced* profile (10 to 100 Mbps, init: 100 Mbps). Section VII employs CBR (100 Mbps) and NeSt-VR’s *Balanced*, *Speedy*, and *Anxious* profiles (10 to 100 Mbps, init: 50 Mbps, for each).

All tests are conducted at 90 fps (and 60 fps in Section IV-B), using our ALVR v20.6.0 fork default settings, including HEVC and UDP. Section VII streams CREW’s XR application (*Anxious Arrivals*¹⁰), while the other sections use

⁶Network delay represents the latency in the motion-to-photon pipeline due to data transmission, including the time required for a tracking packet to travel in the UL and a complete VF —fragmented into multiple packets— to travel in the DL

⁷<https://man7.org/linux/man-pages/man8/tc.8.html>

⁸<https://iperf.fr>

⁹Setting B_{init} to B_{max} ensures video quality equivalent to a B_{max} CBR under optimal network conditions

¹⁰<https://crew.brussels/en/productions/anxious-arrivals>

TABLE I: UPF’s lab equipment details.

1x PC (vr)	OS	Windows 10 x64
	GPU	NVIDIA GeForce RTX 3080, 10 GB
	CPU	i5-12600KF
2x Laptop	Model	Dell G15 5521
	OS	Windows 11 x64
	GPU	NVIDIA GeForce RTX 3060 Mobile
1x PC (netem)	CPU	i7-12700H
	Model	Dell Optiplex 3000
	OS	Ubuntu Desktop 22.04.3
1x AP (vr)	GPU	Intel UHD Graphics 770
	CPU	i5-12500
	Model	ASUS ROG Rapture GT-AXE11000
1x AP (udp)	Standard	802.11ax
	Model	ASUS TUF-AX4200
	Firmware	OpenWrt 23.05.5
2x HMD	Standard	802.11ax
	Model	Meta Quest 2

TABLE II: CREW’s equipment details.

2x PC	OS	Windows 11 x64
	GPU	NVIDIA GeForce RTX 4090
	CPU	i9-12900K
1x AP	Model	Netgear Nighthawk RAXE500
	Standard	802.11ax
2x HMD	Model	HTC Vive Focus 3

TABLE III: Test configurations. C: CBR, A: *Adaptive*, N: NeSt-VR (b: *Balanced*, s: *Speedy*, x: *Anxious*).

section	setup	time (s)	fps	OBSS	C	A	N
IV-B	(a)	~30	90, 60	×	✓	×	×
V	(a)	~70	90	×	✓	×	×
VI-A	(a)	~120	90	×	✓	✓	b
VI-B	(a)	~120	90	×	✓	×	b
VI-C	(b)	~120	90	×	✓	×	b
VI-D	(c)	~30	90	✓	✓	×	b
VII	-	~140	90	×	✓	×	b, s, x

SteamVR Home. Tbl. III summarizes the test configurations across our sections.

C. Datasets

Our dataset, publicly available on Zenodo¹¹, contains ALVR session logs (.json) with statistics, for each test in Sections V and VI. Additionally, for each test in Section V, it includes *tshark*-processed traffic traces (.csv) collected using WireShark v4.0.3 at both the server and the netem’s Ethernet interface to the AP. Note that there is no packet capture application available for a Meta Quest 2. Thus, the server’s interface captures the generated video packet stream and the UL packets received, while the netem’s interface captures the stream after the emulation of network effects.

IV. NESt-VR AND WN-ALVR EXTENSIONS

We have created an ALVR fork that incorporates several network performance metrics, aiding the decision-making process

of any ABR algorithm. For instance, metrics like the arrival span and inter-arrival time of VFs can be used to replicate VR-specific ABR algorithms such as EVerEst [13], [14].

Modifications have been made throughout ALVR’s pipeline to gather client-side statistics—essential for obtaining the network performance metrics of interest—and relay them to the server for their logging and utilization in our implemented ABR algorithm, NeSt-VR. Notably, since ALVR may drop decoded VFs prior to visualization if the queue of decoded frames overflows, thereby preventing the transmission of their associated native statistics packets, our client-side statistics are encapsulated in an additional 56-byte UL packet. This packet is sent over TCP in the UL immediately after the client receives a VF. Hence, for a given VF, the feedback is received at the server significantly sooner than using ALVR’s native statistics packet, which is delayed until the VF is ready for display.

A. Characterizing Network Performance

Here, we introduce the new performance metrics integrated into ALVR to gather information about the network’s performance, using the notation summarized in Tables IV and V.

1) Time-related metrics:

- **Client-side frame span** (Δt_f^-): time required to receive all packets of frame f at the client:

$$\Delta t_f^- = \max_{n \in \{1, \dots, N_f\}} t_{n,f}^- - \min_{n \in \{1, \dots, N_f\}} t_{n,f}^- \quad (1)$$

- **Frame inter-arrival time** ($\Delta t_{f,f_1}^-$): time interval between the complete reception of frames f and f_1 . It is indicative of the network’s consistency in delivering VFs:

$$\Delta t_{f,f_1}^- = \max_{n \in \{1, \dots, N_f\}} t_{n,f}^- - \max_{n \in \{1, \dots, N_{f_1}\}} t_{n,f_1}^- \quad (2)$$

- **Video Frame Round-Trip Time** (VF-RTT $_f$): time it takes for frame f to travel from the server to the client and for our supplementary UL packet ($P_{\text{stats},f}$)—promptly sent upon the complete reception of the VF—to reach the server:

$$\text{VF-RTT}_f = T_{\text{stats},f}^- - T_{1,f}^+ \quad (3)$$

2) Reliability metrics:

- **Packet loss** (PL $_{f,f_1}$): number of packets lost in the interval between the complete reception of frames f and f_1 :

$$\text{PL}_{f,f_1} = N_{f,f_1}^e - N_{f,f_1}^-, \quad (4)$$

where $N_{f,f_1}^- = |\mathcal{P}_{f,f_1}|$ represents the number of packets received and $N_{f,f_1}^e = \text{hseq}_f - \text{hseq}_{f_1}$ represents the anticipated number packets to be received during the interval. Thus, packet loss ratio (PLR) is given by $\text{PLR}_{f,f_1} = \text{PL}_{f,f_1} / N_{f,f_1}^e$.

3) Data rate metrics:

- **Instantaneous video network throughput** (Th $_{f,f_1}$): rate at which video packet data (including headers and prefixes) is received at the client in the interval between the complete reception of frames f and f_1 . It reflects the

¹¹<https://doi.org/10.5281/zenodo.14832268>

network's capability to sustain the desired video quality according to the encoder's target bitrate:

$$\text{Th}_{f,f_1} = \frac{\sum_{\forall P_{n',f'} \in \mathcal{P}_{f,f_1}} L_{P_{n',f'}}}{\Delta t_{f,f_1}^-} \quad (5)$$

- **Peak network throughput** ($\text{Th}_f^{\text{peak}}$): rate at which video packet data (including headers and prefixes) from frame f is received at the client. It serves as an estimate of the network capacity since ALVR sends each VF in a single burst:

$$\text{Th}_f^{\text{peak}} = \frac{L_f}{\Delta t_f^-}, \quad (6)$$

4) Network Stability metrics:

- **VF jitter** (FJ_f): variability in VF time deliveries, providing insight into the smoothness of video playback. It is computed as the sample standard deviation of frame inter-arrival times over a sliding window of w frames:

$$\text{FJ}_f = \sqrt{\frac{1}{w-1} \sum_{f'=f-w+1}^f \left(\Delta t_{f',f_1}^- - \overline{\Delta t} \right)^2}, \quad (7)$$

where f is the most recently received frame and $\overline{\Delta t}$ is the mean inter-arrival time over the window of w frames,

$$\text{i.e., } \overline{\Delta t} = \frac{1}{w} \sum_{f'=f-w+1}^f \Delta t_{f',f_1}^-.$$

- **Video packet jitter** (PJ_f): variability in video packet arrival times, providing insight into the consistency of packet delivery. As defined and formulated in RFC 3550 [16], the packet inter-arrival jitter at the reception of packet P_n (PJ_n) is the mean deviation of the difference D in packet spacing at the receiver compared to the sender for packets P_n and P_{n_1} :

$$\text{PJ}_n = \text{PJ}_{n_1} + (|D_{n,n_1}| - \text{PJ}_{n_1})/16 \quad (8)$$

where $D_{n,n_1} = (t_n^- - t_{n_1}^-) - (T_n^+ - T_{n_1}^+)$.

Thus, PJ_f is derived from the jitter value PJ_n of the latest packet that completes frame f .

- **Filtered one-way delay gradient** (FOWD_f)¹²: rate of change in one-way delay between frames f and f_1 (OWD_{f,f_1}), smoothed using a Kalman filter as described in [12] and a state noise variance of 10^{-7} :

$$\text{OWD}_{f,f_1} = \Delta t_{f,f_1}^- - (T_{1,f}^+ - T_{1,f_1}^+) \quad (9)$$

¹²FOWD is used in delay-based congestion control algorithms such as Google Congestion Control (GCC) [12]

¹³Note that T refers to server time and t refers to client time. $+$ indicates transmission and $-$ indicates reception

¹⁴Note that the order of transmission may differ from the order of arrival if packet reordering occurs

¹⁵If the frame transmitted prior to frame f (i.e., $f-1$) is not lost, skipped, or delayed, then $f_1 = f-1$

¹⁶The departure time of each packet ($T_{n,f}^+$) has been incorporated into each packet application prefix

¹⁷The sequence number serves as a unique identifier for each packet within the global sequence of transmitted packets

TABLE IV: Support notation¹³.

Symbol	Description
N_f	number of packets in the f -th frame transmitted
$P_{n,f}$	n -th packet transmitted of frame f ¹⁴
$P_{\text{stats},f}$	statistics packet associated to frame f
f_{-1}	frame received immediately before frame f ¹⁵
P_{n-1}	video packet received immediately before packet P_n
L_h, L_q	(bits) transport header and application prefix size
$L_{v_{n,f}}$	(bits) payload size of packet $P_{n,f}$
$L_{P_{n,f}}$	(bits) total size of packet $P_{n,f}$: $L_h + L_q + L_{v_{n,f}}$
L_{v_f}	(bits) payload size of frame f : $\sum_{n=1}^{N_f} L_{v_{n,f}}$
L_f	(bits) total size of frame f : $\sum_{n=1}^{N_f} L_{P_{n,f}}$
$T_{n,f}^+$	departure time of $P_{n,f}$ from server ¹⁶
$t_{n,f}^-$	arrival time of $P_{n,f}$ at client
$T_{\text{stats},f}^-$	arrival time of $P_{\text{stats},f}$ at server
$\text{seq}_{n,f}$	sequence number ¹⁷ of packet $P_{n,f}$: $n + \sum_{f'=1}^{f-1} N_{f'}$
hseq_f	highest sequence number at completion of frame f
\mathcal{P}_{f,f_1}	set of packets received in the interval between frames f and f_1
N_{f,f_1}^e	number of expected packets in the interval between frames f and f_1
N_{f,f_1}^-	number of received packets in the interval between frames f and f_1

TABLE V: Network metrics notation.

Symbol	Description
Δt_f^-	client-side frame span for frame f
$\Delta t_{f,f_1}^-$	client-side inter-arrival time between frames f and f_1
RTT_f	round-trip time for frame f
PL_{f,f_1}	packet loss between between frame f and frame f_1
Th_{f,f_1}	throughput over the interval between frames f and f_1
$\text{Th}_f^{\text{peak}}$	throughput measured for frame f
FJ_f, PJ_f	video frame and video packet jitter at the reception of frame f
OWD_{f,f_1}	one-way delay gradient between frames f and f_1

B. NeSt-VR

NeSt-VR is a configurable ABR algorithm designed to dynamically adjust the video bitrate in response to network congestion intervals during the streaming of VR content over Wi-Fi. Given that network congestion introduces delays and losses that significantly disrupt the reception of VFs, NeSt-VR relies on the Network Frame Ratio (NFR) and VF-RTT. These metrics are averaged ($\bar{\cdot}$) to avoid overreacting to severe but sporadic congestion episodes. The averaging method is configurable and supports a sliding window of n samples, a sliding window of t seconds (defaulting to τ), or an Exponentially Weighted Moving Average (EWMA) with weight ω .

NFR is indicative of the network's reliability and consistency in delivering VFs, and is given by $\overline{\text{NFR}} = \overline{\text{fps}_{\text{rx}}/\text{fps}_{\text{tx}}}$, where fps_{rx} and fps_{tx} denote the frame delivery rate¹⁸ and frame transmission rate, respectively. Here, $\overline{\text{fps}_{\text{rx}}} = 1/\overline{\Delta_{\text{rx}}}$ and $\overline{\text{fps}_{\text{tx}}} = 1/\overline{\Delta_{\text{tx}}}$, where Δ_{rx} ¹⁹ and Δ_{tx} ²⁰ denote the intervals between consecutive VFs receptions and transmissions, respectively.

As described in Algorithm 1, NeSt-VR operates every τ seconds, progressively adjusting the target bitrate ($B_k \in \mathcal{B}$) in discrete steps to avoid significant video quality shifts that may disrupt the user's QoE. The set of available target bitrates (\mathcal{B}) depends on the configured minimum bitrate (B_{\min}), maximum bitrate (B_{\max}), and the number of steps between them ($N_s \in \mathbb{Z}^+$): $\mathcal{B} = \{B_{\min} + i \cdot \Delta B \mid i = 0, 1, \dots, N_s\}$ where $\Delta B = (B_{\max} - B_{\min})/N_s$ is the step size. Thus, the computational complexity of determining the target bitrate B_k is $\mathcal{O}(N_s)$. At each adjustment period $k \in \mathbb{Z}^+$, occurring at time $T = k \cdot \tau$, NeSt-VR computes the average NFR and average VF-RTT, and applies a hierarchical decision-making process:

- If the average NFR is below its threshold ρ , the target bitrate—and consequently, also the number of packets per VF—is reduced in $N_{\text{dw}} \in \mathbb{Z}^+$ steps to reduce bandwidth utilization, minimizing packet losses and enhancing the frame delivery rate.
- If both the average NFR and average VF-RTT surpass their thresholds (ρ and σ , respectively), it indicates an adequate VF delivery rate but significant delay in VF arrivals, potentially impacting motion-to-photon latency. Thus, with a probability of γ_{rtt} ²¹, the bitrate is reduced in $N_{\text{dw}} \in \mathbb{Z}^+$ steps; otherwise, it remains consistent.
- If the average NFR exceeds ρ and the average VF-RTT is below its threshold σ , the network may be capable of sustaining a higher bitrate. Thus, with probability γ_+ ²², the bitrate is increased in $N_{\text{up}} \in \mathbb{Z}^+$ steps; otherwise, it remains consistent.
- Finally, to ensure the bitrate does not exceed the network's capacity, the target bitrate is upper-bounded by $m \cdot C_{\text{NeSt-VR}}$, with $m \leq 1$. Here, $C_{\text{NeSt-VR}}$ denotes NeSt-VR's estimated network capacity, computed as the average of the peak network throughput (Th^{peak}).

Tbl. VI summarizes NeSt-VR's configurable parameters and Tbl. VIIa outlines our parameter recommendations: $\tau = 1$ s balances responsiveness and stability; a sliding window of $t = 1$ s (i.e., $t = \tau$) filters short-term fluctuations and ensures adaptation based on the network's response to the latest bitrate decision; $m = 0.9$ provides a safety margin, preventing the bitrate from exceeding the network's capacity;

¹⁸Frame delivery rate denotes the frames per second successfully and timely received at the client after network transmission

¹⁹Note that Δ_{rx} is equivalent to the frame inter-arrival time ($\Delta t_{f,f-1}^-$)

²⁰Note that Δ_{tx} is equivalent to the frame inter-departure time ($\Delta T_{f,f-1}^+$), where $\Delta T_{f,f-1}^+ = \max_{n \in \{1, \dots, N_f\}} T_{n,f}^+ - \max_{n \in \{1, \dots, N_f-1\}} T_{n,f-1}^+$

²¹ γ_{rtt} moderates the frequency of bitrate reductions in response to a high average VF-RTTs, particularly when frame delivery rates are acceptable, thereby giving greater weight to NFR over VF-RTT in bitrate adaptation decisions

²² γ_+ serves as an exploration parameter to assess whether higher bitrates can be sustained without compromising the user's QoE

Algorithm 1: NeSt-VR

Input: $B_{\min}, B_{\max}, B_{\text{init}}, N_s, N_{\text{up}}, N_{\text{dw}}, \tau, m, \rho, \sigma, \gamma_+, \gamma_{\text{rtt}}$
Output: Target bitrate sequence $\{B_k\}$

- 1 $\Delta B \leftarrow (B_{\max} - B_{\min})/N_s$;
- 2 $\mathcal{B} \leftarrow \{B_{\min}, B_{\min} + \Delta B, B_{\min} + 2\Delta B, \dots, B_{\max}\}$;
- 3 $B_0 \leftarrow \max\{B \in \mathcal{B} \mid B \leq \max(B_{\text{init}}, B_{\min})\}$;
- 4 **for** each adjustment period $k \geq 1$, at $T = k \cdot \tau$ **do**
- 5 Compute avg. NFR, avg. VF-RTT, and $C_{\text{NeSt-VR}}$;
- 6 **if** avg. NFR $< \rho$ **then**
- 7 $B_k \leftarrow \max(B_{\min}, B_{k-1} - N_{\text{dw}} \cdot \Delta B)$; { - }
- 8 **else**
- 9 **if** avg. VF-RTT $> \sigma$ **then**
- 10 Sample $r_{\text{rtt}} \sim \mathcal{U}(0, 1)$;
- 11 **if** $r_{\text{rtt}} \leq \gamma_{\text{rtt}}$ **then**
- 12 $B_k \leftarrow \max(B_{\min}, B_{k-1} - N_{\text{dw}} \cdot \Delta B)$; { - }
- 13 **else**
- 14 $B_k \leftarrow B_{k-1}$; { = }
- 15 **else**
- 16 Sample $r_+ \sim \mathcal{U}(0, 1)$;
- 17 **if** $r_+ \leq \gamma_+$ **then**
- 18 $B_k \leftarrow \min(B_{\max}, B_{k-1} + N_{\text{up}} \cdot \Delta B)$; { + }
- 19 **else**
- 20 $B_k \leftarrow B_{k-1}$; { = }
- 21 $B_k \leftarrow \max\{B \in \mathcal{B} \mid B \leq \max(m \cdot C_{\text{NeSt-VR}}, B_{\min})\}$
- 22 Output B_k ;

TABLE VI: NeSt-VR parameters.

Adjustment interval (s)	τ	Averaging param.	$n/t/\omega$
Est. capacity multiplier	m	min, max Bitrate	B_{\min}, B_{\max}
VF-RTT thresh. (ms)	σ	initial Bitrate	B_{init}
NFR thresh.	ρ	Bitrate steps count	N_s
VF-RTT adj. prob.	γ_{rtt}	Bitrate inc. steps	N_{up}
Bitrate inc. explor. prob.	γ_+	Bitrate dec. steps	N_{dw}

TABLE VII: NeSt-VR parameter recommendations and profiles.

(a) Recommendations.					(b) Profiles overview.		
τ	1	σ	22	ρ	0.99	(b) <i>Balanced</i>	$N_{\text{dw}} = N_{\text{up}}$
t	1	γ_{rtt}	1	γ_+	0.25	(s) <i>Speedy</i>	$N_{\text{dw}} = 2N_{\text{up}}$
m	0.9	N_s	9	N_{up}	1	(x) <i>Anxious</i>	$N_{\text{dw}} = N_s$

$\rho = 0.99$ and $\sigma = 22$ ms ensure positive user experiences²³, as outlined in Tbl. VIII; $\gamma_{\text{rtt}} = 1$ guarantees that the bitrate is reduced whenever significant delays in VF arrivals are detected; $\gamma_+ = 0.25$ ensures a cautious exploration of higher bitrates; $N_s = 9$ offers granularity in bitrate adaptation; and $N_{\text{up}} = 1$ ensures gradual bitrate increases. Tbl. VIIb highlights our predefined profiles: *Balanced* (consistent increase and decrease adjustments), *Speedy* (faster bitrate reductions), and *Anxious* (bitrate drops to the minimum). These profiles integrate our parameter recommendations and can be selected based on the desired responsiveness to network fluctuations. Note that parameters such as $B_{\min}, B_{\max}, B_{\text{init}}$ depend on the quality requirements of the target application.

²³Our thresholds are in line with ITU-T recommendations (RTT around 20 ms and packet loss $\leq 1e-5$) [17], [18], as, in our tests, packet loss rates of $1e-5$ and $1e-6$ consistently resulted in NFRs above 0.99

TABLE VIII: Authors’ satisfaction in terms of average NFR and average VF-RTT under emulated packet loss (from 1e-3 to 1e-6) and network delays (from 6 to 40 ms). VF-RTT in standard conditions was 4-5 ms. ✗ (or ✘) indicates that all (or only some) authors perceived visual artifacts (e.g., pixelation, blurring), black borders, or lag in the video. ✓ indicates no observed impairments.

NFR	0.91	0.99	0.999	VF-RTT	11	16	22	33	44
60 fps	✗	✓	✓	60 fps	✓	✓	✓	✘	✗
90 fps	✗	✓	✓	90 fps	✓	✓	✓	✓	✘

V. METRICS VALIDATION

The metrics introduced in Section IV-A have been independently compared against their measured counterparts derived from parsed Wireshark traffic traces²⁴ to assess their reliability and representativeness. In particular, the application prefix within each packet’s payload has been parsed to identify VFs and the metrics have been computed independently but in an analogous manner to ALVR —logging metrics only for completely and timely received VFs.

Several single-user tests have been conducted, emulating individual network effects: *i*) limited bandwidth; *ii*) packet loss; *iii*) duplicated packets; and *iv*) packet-level jitter. Each test comprised three 10-second intervals of emulated effects at varying intensities, interspersed with 10-second intervals in normal conditions. Note that using netem’s Wireshark traces leads to optimistic measurements, as it does not account for Wi-Fi transmission delays.²⁵ Thus, to minimize the Wi-Fi’s hop impact on packet timings, the client was positioned close to the AP (<1 m) with a Received Signal Strength Indicator (RSSI) of -40 dBm. The specific emulation effects and their levels at each interval are detailed in Tbl. IX. Due to space constraints, in this paper, we present only our results from test *i*) (limited bandwidth). Validation results for other scenarios are available in Zenodo¹¹.

Fig. 5 demonstrates that both the metrics logged within ALVR and their measurements derived from Wireshark traces exhibit similar distributions. However, as illustrated in Figs. 5a and 5b, both the client-side frame span and peak network throughput differ under baseline conditions. This disparity can be attributed to Wi-Fi’s lower data rate compared to Ethernet’s 1 Gbps link, highlighting Wi-Fi as the system’s bottleneck when the bandwidth limitation in the netem is not enforced.

Fig. 5b illustrates that peak network throughput is an effective estimator of network capacity during bandwidth-limited periods. Concurrently, there are significant increases in client-side frame span and VF-RTT due to the traffic controller limiting the packet departure rate. Additionally, substantial packet losses occur as the first-in-first-out queue of the netem overflows, leading to increased frame inter-arrival

²⁴Netem traffic traces were employed to validate frame span, frame inter-arrival, and network throughput, while server traces were used to validate VF-RTT. Both netem and server traces contributed to validate PL and FOWD

²⁵Discrepancies between results from netem Wireshark traces and ALVR logs can be used to isolate the Wi-Fi impact on the system’s network performance

TABLE IX: Emulated network effects and their intensities.

		Interval 1	Interval 2	Interval 3
1	Lim. bandwidth	100 Mbps	95 Mbps	90 Mbps
2	Packet loss	0.5%	1%	2%
3	Duplicated pkts	0.5%	1%	2%
4	Packet jitter	0-6 ms	0-10 ms	0-20 ms

times. During transition periods, there are noticeable peaks in FOWD as the netem’s packet departure rate to the AP varies.

VI. NeSt-VR: PERFORMANCE ASSESSMENT

Section VI-A compares the operation, behavior, and performance of CBR, *Adaptive*, and NeSt-VR during an emulated bandwidth-limited single-user test. On the other hand, Sections VI-B, VI-C, and VI-D evaluate NeSt-VR’s performance (compared to CBR) in diverse real-world scenarios. In particular, Section VI-B introduces mobility and explores how RSSI reductions —caused by moving farther from the AP— impact a single user’s VR streaming. Section VI-C introduces a second user to increase network demand and assess NeSt-VR’s effectiveness in a multi-user environment. Lastly, Section VI-D investigates a single-user scenario with OBSS activity. Performance is assessed based on the target bitrate and key QoS metrics: frame delivery rate, packet loss, and VF-RTT. Note that, during all tests, the server(s) consistently achieved a transmission frame rate of 90 fps.

A. Network capacity fluctuations

During this test, the network capacity changes during three 20-second intervals. Between intervals, there are 20 seconds under normal network conditions. As in Section V, the bandwidth is limited to the values outlined in Tbl. IX and the client is approximately placed 1 m from the AP, observing a -40 dBm RSSI. CBR, *Adaptive*, and NeSt-VR performance across each bandwidth-limited interval is summarized in Tbl. X.

As depicted in Fig. 6a, CBR maintains a constant 100 Mbps target bitrate regardless of the network’s capacity. As detailed in Tbl. Xa, this leads to VF-RTTs above 90 ms and substantial packet losses during bandwidth-limited periods, resulting in a significant reduction in frame delivery rate.

In contrast, as illustrated in Fig. 6b, *Adaptive* rapidly decreases the target bitrate to the minimum (i.e., 10 Mbps) in response to increased delays stemming from constraining the network capacity. Then, since drastically reducing the bitrate leads to much smaller VFs, which in turn decreases network delay and VF-RTT, the algorithm starts increasing the target bitrate until stabilization around 60 Mbps, as outlined in Tbl. Xb. Once the bandwidth limitation is deactivated, *Adaptive* promptly increases the target to the maximum (i.e., 100 Mbps). Thus, as illustrated, *Adaptive* is able to adapt the bitrate when capacity changes, reducing VF-RTTs, minimizing

²⁵Average video network throughput is computed using a time-weighted average of instantaneous throughput values rather than an arithmetical average given non-uniform intervals between samples

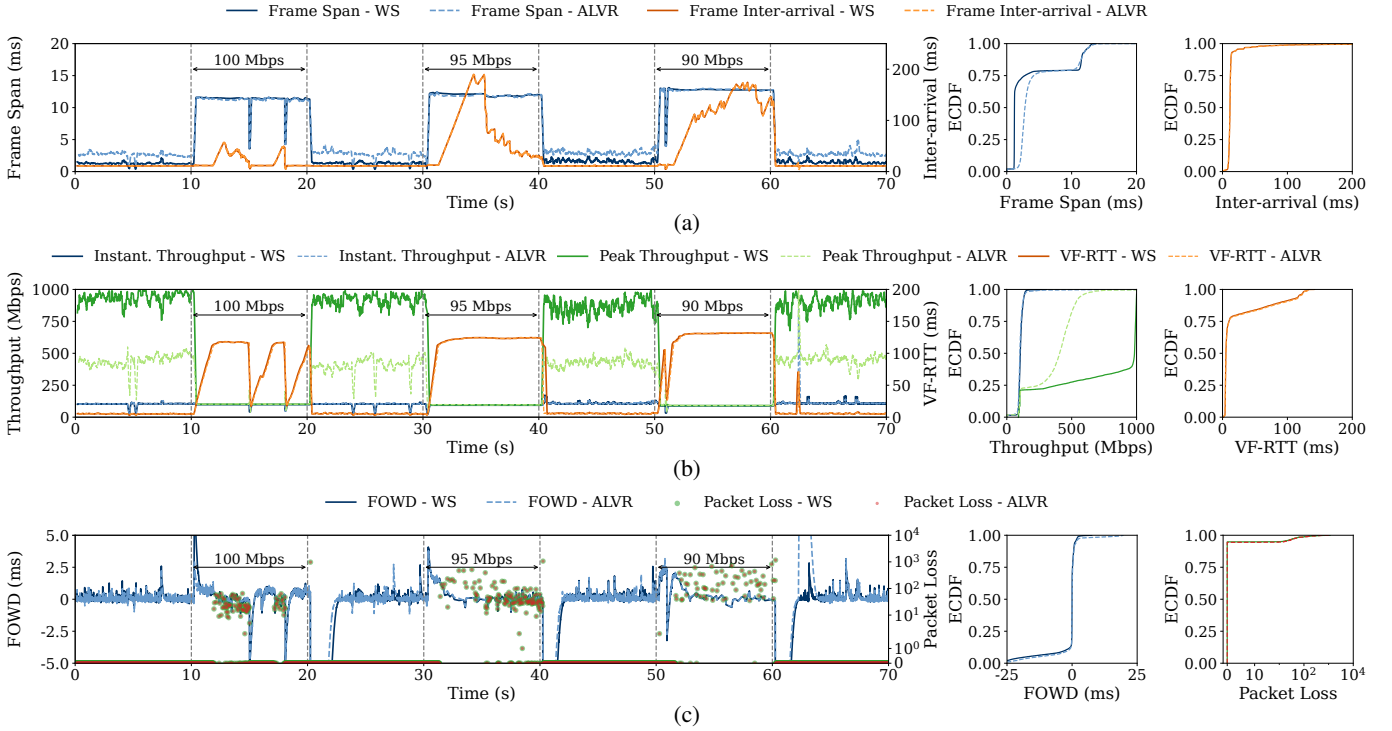


Fig. 5: Temporal evolution and Empirical Cumulative Distribution Functions (ECDF) of our metrics under a bandwidth-limited test (see 1 in Tbl. IX), comparing the values logged in ALVR with those independently derived from Wireshark (WS) traces. Temporal evolutions are filtered using a 16-sample sliding window average to enhance visibility, except for packet loss (discrete) and FOWD (implicitly filtered).

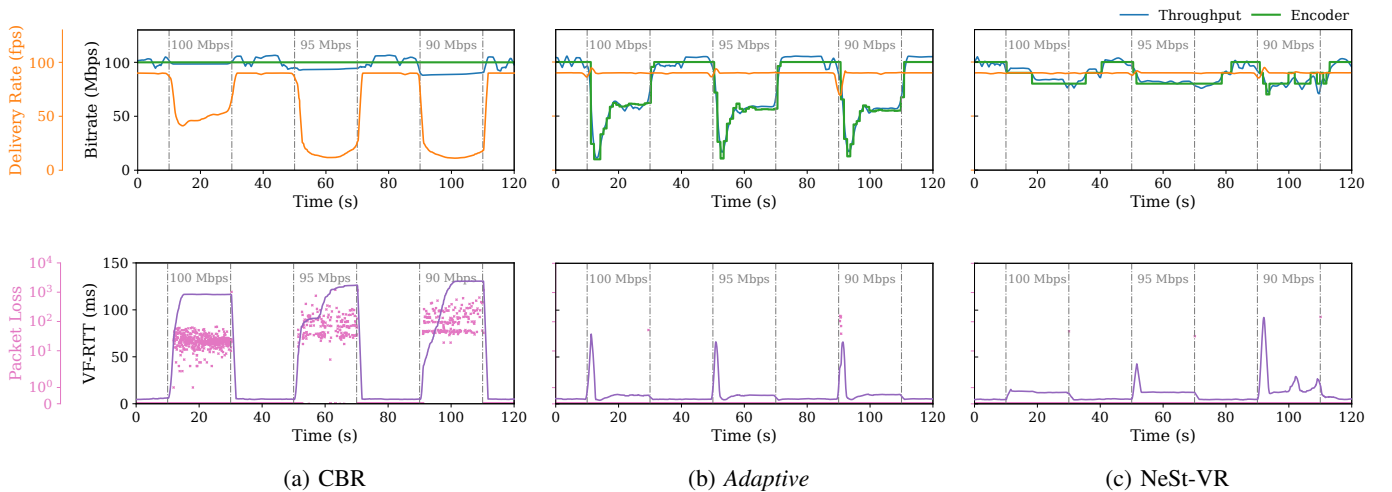


Fig. 6: Comparison of CBR, *Adaptive*, and NeSt-VR under emulated limited bandwidth conditions. Sliding window of 128 samples for frame delivery rate, average video network throughput²⁵, and VF-RTT.

packet losses²⁶ and maintaining high frame delivery rates, as detailed in Tbl. Xb.

Similarly, as shown in Fig. 6c, NeSt-VR is able to react to capacity changes, ensuring the target bitrate remains below the network capacity. Instead of dropping the target bitrate to the minimum, it is progressively reduced in $\Delta B = 10$ Mbps

steps. These adjustments are triggered at the beginning of the emulated effects, due to reduced frame delivery rates (NFR below ρ) and increased VF-RTTs (above σ ms). Upon removal of each limit in bandwidth, NeSt-VR increases the target bitrate (with probability γ_+) in ΔB steps, taking a more conservative approach to maintain consistent image quality. This behavior leads to higher target bitrates than *Adaptive* at each interval, while also sustaining low VF-RTTs, high frame delivery rates, and minimal packet losses²⁶, as detailed

²⁶Packet loss occurs because deleting the netem's `tc` queueing discipline (`qdisc`) causes any queued packets to be dropped. Consequently, frame losses occur, reducing the frame delivery rate

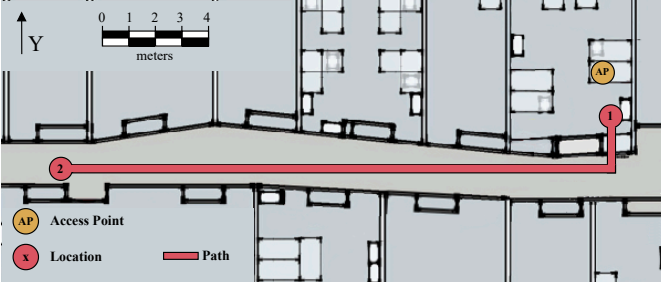


Fig. 7: UPF’s lab floor plan. *User A* travels from *Location 1* to *Location 2* in ~ 40 seconds, remains stationary at *Location 2* for ~ 40 seconds, and returns to *Location 1* in ~ 40 seconds. *User B* remains stationary at *Location 2* throughout the test.

in Tbl. Xc.

Thus, *Adaptive* drastically reduces bitrate under congestion, causing abrupt drops. In contrast, NeSt-VR —except in its most aggressive mode (*Anxious* profile)— adjusts bitrate gradually, avoiding excessive reductions, and prevents bitrate overshooting by leveraging a validated capacity estimation.

B. Testing Wi-Fi performance limits: a Mobility case

To assess a situation in which a single AP approaches its capacity to effectively serve one user, we conduct a mobility test where *User A* moves between *Location 1* (RSSI -48 dBm, i.e., near the AP) and *Location 2* (RSSI -78 dBm, i.e., far from the AP) at a leisurely walking pace. Fig.7 illustrates the layout and *User A*’s mobility path.

As detailed in Tbl. XIa, using CBR, the significant reduction in RSSI at *Location 2* —the farthest point from the AP— and the subsequent decline in Wi-Fi transmission rates lead to periods of network instability, causing occasional packet loss and VF-RTTs exceeding 40 ms. In contrast, as outlined in Tbl. XIb, NeSt-VR effectively responds to increased network delays by momentarily reducing the target bitrate by a single step, thereby minimizing packet loss and maintaining VF-RTTs at lower levels. Fig. 8a shows that NeSt-VR yields smaller VF-RTTs than CBR for *User A*.

Thus, at *Location 2*, the AP begins to struggle to maintain stable performance with a 100 Mbps bitrate. Hence, in the next section, we position a stationary user at *Location 2* and introduce a second, moving user to assess the impact of increased network demand on both users’ VR streaming performance.

C. Multiple users

In this multi-user scenario, *User A* follows the same mobility pattern as described in Section VI-B, while a second user, *User B*, remains stationary at *Location 2* throughout the 120-second test. Note that the presence of a user farther from the AP degrades the performance of nearer users due to the so-called *Performance Anomaly* [19], as demonstrated in [20].

To assess impact on each user’s performance, let us first establish performance baselines using CBR. In particular, let us consider: a) *User A*, moving between *Location 1* and

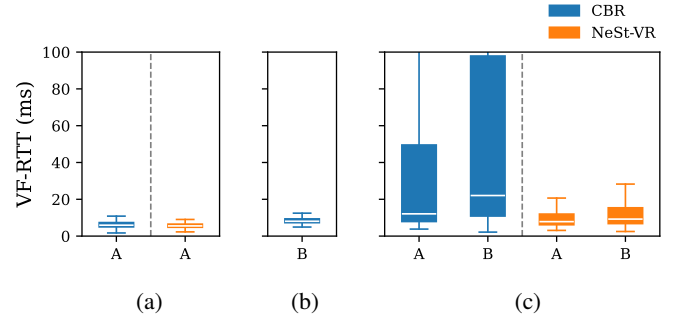


Fig. 8: VF-RTT distribution for (a) *User A* in isolation, (b) *User B* in isolation, and (c) both *User A* and *User B* in a multi-user test, using CBR and NeSt-VR’s *Balanced* profile. Note that for (b) results are shown only for CBR, as NeSt-VR maintained a constant target bitrate throughout the test.

Location 2, in isolation (refer to Section VI-B); and b) *User B*, stationary at *Location 2*, in isolation. Tbl. XIa and XIb summarize both users’ performance, and Fig. 8a and 8b present their VF-RTT distributions as reference baselines, highlighting that both users experience similar average VF-RTTs in isolation.

Building upon these baseline results, Tbl. XIIa and XIIb detail each user’s performance during the multi-user test for both CBR and NeSt-VR, respectively.

As summarized in Tbl. XIIa, using CBR, performance degrades substantially for both users, especially during interval 2, as both users are farther from the AP (i.e., at *Location 2*) and their MCSs —and thus, transmission rates— are reduced. This is evidenced by extremely high VF-RTTs, severe packet loss (0.32% and 0.12% for *User A* and *B*, respectively), and a drastic reduction in frame delivery rates. Notably, during this interval, *User A* experiences even momentary disconnections and its performance is significantly worse than *User B*’s. However, in intervals 1 and 3, *User A* experiences lower VF-RTTs compared to *User B* but both users sustain high frame rates without packet loss.

Conversely, Tbl. XIIb demonstrates that NeSt-VR maintains consistently a high performance: VF-RTTs remain low, frame delivery rates are high, and no packet loss is observed. In terms of bitrate adaptation, NeSt-VR dynamically adjusts the target bitrate for both users across intervals but particularly during interval 2. Notably, *User B*’s target bitrate is consistently lower than *User A*’s. This is because, during interval 1, *User A* requires fewer bitrate adjustments, as its VF-RTTs are closer to the established 22 ms threshold. As a result, at the start of interval 2, *User A*’s bitrate is significantly higher than *User B*’s. Thus, since both users adjust their bitrate every second in equal steps, once the network is no longer congested, *User A*’s target bitrate is higher. On the other hand, during interval 3, as network conditions stabilize and become favorable, enhancing both users’ performance, bitrates are increased conservatively. Likewise, *User A*’s bitrate remains higher due to its bitrate being greater at the start of the interval.

Fig. 8c clearly demonstrates that CBR leads to higher VF-RTTs for both users compared to NeSt-VR, with VF-

TABLE X: CBR, *Adaptive*, and NeSt-VR performance results under emulated limited bandwidth conditions. VF-RTT: Video Frame Round-Trip Time; FDR: frame delivery rate; PL: total packets lost. BR: target bitrate. Results are provided for three intervals of limited bandwidth (1: 100 Mbps, 2: 95 Mbps, and 3: 90 Mbps).

(a) CBR				
	VF-RTT (ms)	FDR (fps)	PL (pkts)	BR (Mbps)
1	107.1 ± 25.5	55.2 ± 14.7	10,598	100 ± 0.0
2	94.6 ± 33.4	51.9 ± 33.4	18,364	100 ± 0.0
3	106.2 ± 43.2	41.8 ± 32.2	26,277	100 ± 0.0

(b) <i>Adaptive</i>				
	VF-RTT (ms)	FDR (fps)	PL (pkts)	BR (Mbps)
1	12.5 ± 18.0	89.9 ± 1.7	52	53.8 ± 20.5
2	11.7 ± 16.4	90.0 ± 1.6	0	54.4 ± 15.4
3	12.0 ± 17.4	88.4 ± 5.5	665	52.5 ± 14.5

(c) NeSt-VR (<i>Balanced</i>)				
	VF-RTT (ms)	FDR (fps)	PL (pkts)	BR (Mbps)
1	12.6 ± 2.0	89.8 ± 0.3	47	84.2 ± 5.1
2	14.5 ± 8.0	90.0 ± 0.8	32	80.9 ± 3.6
3	22.6 ± 21.7	90.0 ± 2.0	147	82.8 ± 6.1

TABLE XI: Performance results for *User A* and *User B* in isolation. VF-RTT: Video Frame Round-Trip Time; FDR: frame delivery rate; PL: total packets lost; . Results for *User A* are provided for three intervals (1: *User A* travels from *Location 1* to 2, 2: *User A* remains at *Location 1*, and 3: *User A* returns to *Location 1*) along with the overall (O) performance. Results for *User B* are presented only in terms of overall (O) performance. Temporal evolution figures for these metrics are available on Zenodo¹¹.

(a) CBR					
		VF-RTT (ms)	FDR (fps)	PL (pkts)	BR (Mbps)
A	O	9.2 ± 18.5	89.8 ± 1.5	369	100 ± 0.0
A	1	6.7 ± 5.2	89.9 ± 0.5	40	100 ± 0.0
A	2	14.8 ± 30.0	89.8 ± 2.5	329	100 ± 0.0
A	3	5.7 ± 3.5	89.9 ± 0.4	0	100 ± 0.0
B	O	9.5 ± 6.2	90.0 ± 0.3	0	100 ± 0.0

(b) NeSt-VR (<i>Balanced</i>)					
		VF-RTT (ms)	FDR (fps)	PL (pkts)	BR (Mbps)
A	O	6.8 ± 6.6	89.8 ± 1.0	24	99.0 ± 3.0
A	1	6.1 ± 5.9	89.9 ± 0.5	24	99.0 ± 3.0
A	2	8.1 ± 8.4	89.9 ± 0.5	0	99.0 ± 2.9
A	3	6.0 ± 4.6	89.5 ± 1.5	0	99.0 ± 3.0

RTTs frequently exceeding 100 ms. For *User B*, VF-RTTs are generally higher and exhibit greater variability compared to *User A*. However, despite a higher median, *User B* exhibits a lower overall mean VF-RTT under CBR, as *User A*'s extreme VF-RTTs spikes elevate the mean.

D. OBSS traffic

OBSS interference arises in dense Wi-Fi deployments when multiple Basic Service Sets (BSSs)²⁷ operate on overlapping channels, causing contention. Since Wi-Fi networks perform a clear channel assessment before transmission, deferring if the radio frequency medium is busy, OBSS interference degrades throughput and increases latency [21], [22] —detrimental to delay-sensitive applications such as VR streaming. Thus, this section examines the impact of OBSS activity on VR streaming performance and assesses NeSt-VR's effectiveness in maintaining performance in such environments.

As detailed in Section III, while VR streaming is ongoing on one BSS (RSSI: -45 dBm), another BSS operates on the same primary channel, with overlapping coverage areas. The tested levels of OBSS activity (i.e., background UDP traffic load) are: 100 Mbps, 200 Mbps, 300 Mbps, and 400 Mbps at 40 MHz; and 200 Mbps, 400 Mbps, 600 Mbps, and 800 Mbps at 80 MHz. Beyond 400 Mbps at 40 MHz, VR streaming using CBR no longer works. As shown in Figs. 9 and 10, NeSt-VR substantially enhances VR streaming performance by reducing VF-RTTs under high OBSS traffic levels (e.g., 300 Mbps and 400 Mbps at 40 MHz, and 800 Mbps at 80 MHz). At lower traffic levels, NeSt-VR maintains a consistent target bitrate of 100 Mbps, as performance remains within acceptable levels. Notably, at 40 MHz, CBR suffers sporadic packet losses at 300 Mbps (0.28%) and recurrent losses at 400 Mbps (15.64%), resulting in frame delivery rates of 89.8 fps ± 3.7 fps and 72.5 fps ± 8.3 fps, respectively. In contrast, NeSt-VR adjusts the target bitrate to 55.0 Mbps ± 10.3 Mbps and to the minimum (10 Mbps), respectively, maintaining a high frame rate and eliminating packet loss. In the 80 MHz, 800 Mbps OBSS scenario, no packet loss occurs under either CBR or NeSt-VR. However, CBR exhibits significantly higher VF-RTTs, whereas NeSt-VR ensures acceptable network delays by adjusting the target bitrate to 35.1 Mbps ± 11.3 Mbps. Thus, high OBSS activity significantly impacts VR streaming, but NeSt-VR mitigates its effects, as reducing the bitrate alleviates contention for the shared medium and prevents network congestion.

VII. USE-CASE: TESTING NESt-VR IN CREW

CREW²⁸ is an innovative arts company that explores the intersection of art, science, and technology, creating immersive XR performances that allow audiences to engage with alternate realities and interact in the (not) here and (not) now.

In CREW's facilities (~12.5x10 m), using their XR application *Anxious Arrivals*, we evaluated NeSt-VR's performance with its distinct profiles in a multi-user mobility scenario. The tests involved two users, *User C* and *User D*, whose movement paths are illustrated in Fig. 11.

Fig. 12a illustrates the VF-RTT and target bitrate distributions for *User C*, using CBR and NeSt-VR profiles; results for *User D* display similar trends. Consistent with Section VI results, CBR exhibits elevated VF-RTTs, underscoring its

²⁷A BSS comprises a single access point and one or more associated stations

²⁸<https://crew.brussels/>

TABLE XII: Multi-user mobility test performance results for *User A* and *User B* using CBR and NeSt-VR. VF-RTT: Video Frame Round-Trip Time; FDR: frame delivery rate; PL: total packets lost; BR: target bitrate. Results are provided for three intervals (1: *User A* travels from *Location 1* to 2, 2: *User A* remains at *Location 1*, and 3: *User A* returns to *Location 1*) along with the overall (O) performance. Temporal evolution figures for these metrics are available on Zenodo¹¹.

(a) CBR					(b) NeSt-VR (<i>Balanced</i>)					
		VF-RTT (ms)	FDR (fps)	PL (pkts)			VF-RTT (ms)	FDR (fps)	PL (pkts)	BR (Mbps)
A	O	83.7 ± 246.6	83.7 ± 16.1	81,943	A	O	13.1 ± 18.5	90.0 ± 1.5	0	81.1 ± 18.1
A	1	20.8 ± 23.9	89.9 ± 1.1	0	A	1	13.2 ± 17.3	89.9 ± 1.3	0	92.4 ± 8.8
A	2	422.0 ± 468.7	52.3 ± 17.9	81,943	A	2	17.9 ± 25.2	90.0 ± 2.1	0	65.1 ± 14.1
A	3	25.4 ± 43.9	90.3 ± 3.2	0	A	3	8.1 ± 4.2	89.9 ± 0.4	0	87.0 ± 16.7
B	O	76.0 ± 117.3	86.6 ± 10.4	41,892	B	O	17.2 ± 30.9	90.0 ± 0.6	0	42.3 ± 21.6
B	1	39.2 ± 55.6	89.9 ± 3.0	0	B	1	21.5 ± 41.9	90.0 ± 0.7	0	62.0 ± 17.5
B	2	166 ± 164.2	79.4 ± 15.8	41,892	B	2	17.0 ± 21.6	90.0 ± 0.7	0	26.3 ± 11.9
B	3	30.8 ± 40.8	90.0 ± 3.6	0	B	3	13.0 ± 25.5	90.0 ± 0.3	0	39.8 ± 17.7

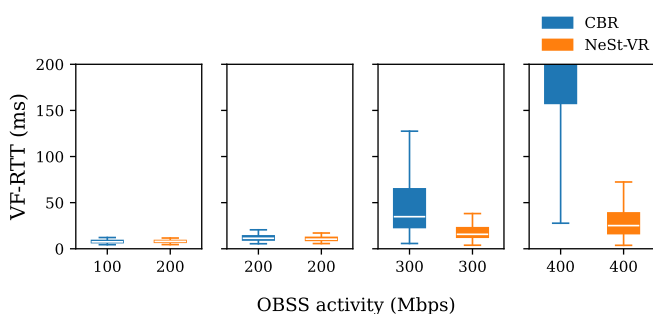


Fig. 9: VR streaming VF-RTT distributions at 40 MHz under distinct OBSS activity levels, using CBR and NeSt-VR’s *Balanced* profile. Note that with CBR and a 400 Mbps OBSS activity, the third quartile (75%) exceeds 400 ms.

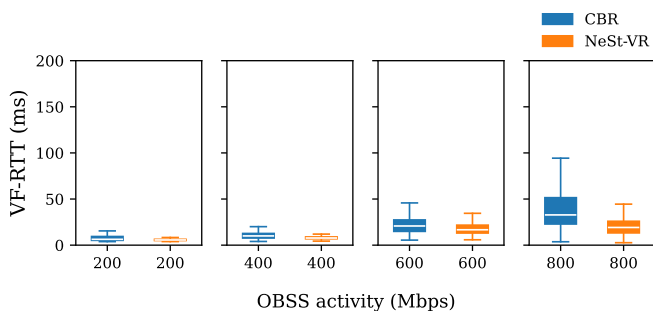


Fig. 10: VR streaming VF-RTT distributions at 80 MHz under distinct OBSS activity levels, using CBR and NeSt-VR’s *Balanced* profile.

inability to adapt to network dynamics. Conversely, NeSt-VR effectively reduces VF-RTTs to acceptable levels. The *Anxious* profile achieves the lowest VF-RTTs by aggressively reducing the bitrate directly to the minimum (10 Mbps). The *Balanced* profile achieves slightly higher VF-RTTs (close to, but not exceeding, the 22 ms threshold for a satisfactory experience) but maintains higher bitrates as its reductions are more gradual, prioritizing consistent quality over rapid adjustments (min. of 30 Mbps). The *Speedy* profile reduces bitrate more rapidly than the *Balanced* profile, resulting in lower VF-RTTs. However, its

coarser granularity leads to lower bitrates (min. of 20 Mbps).

Figs. 12b and 12c display the target bitrate evolution for the *Speedy* and *Anxious* profiles, respectively, highlighting their respective bitrate reduction strategies (see Section IV-B). Notably, bitrate reductions are triggered when users reach locations farther from the AP (i.e., *Location 2* or *3*) if the current bitrate exceeds the network’s capacity (e.g., at the first and third times users reach a distant location). As path loss increases due to greater distance from the AP, a lower signal-to-noise ratio reduces MCS rates and transmission efficiency, prompting NeSt-VR to dynamically adjust the bitrate. Thus, NeSt-VR profiles effectively adapt to deteriorating network conditions, ensuring stable performance despite mobility.

In addition to the multi-user tests, we conducted some single-user tests to evaluate whether the 6 GHz band provides better performance than the 5 GHz band. In general, the 6 GHz band is currently less congested, and given that OBSS activity degrades VR streaming performance (as discussed in Section VI-D), better results should be obtained. Fig. 13 confirms our expectations, showing substantially lower VF-RTTs in the 6 GHz band. Notably, at 5 GHz, VF-RTTs rise rapidly with increasing target bitrates, whereas at 6 GHz, the escalation is much slower.

VIII. RELATED WORK AND DISCUSSION

A. Adaptive Bitrate solutions

ABR implementations vary widely across the literature [23], as they are often designed for specific applications, such as video-on-demand streaming or real-time videoconferencing. Given the unique demands of interactive VR streaming—including stringent latency requirements—traditional buffer-based ABR algorithms such as [24], [11], which perform nearly optimally for pre-buffered video, are ineffective in this context, as exposed in [14]. Consequently, ABR solutions that rely on network bandwidth estimation are a feasible choice for VR streaming. Network bandwidth estimation can be performed through direct packet probing, which introduces overhead [25], deep neural network [26] models based on network features (e.g., [27]), or throughput-based inference from received data chunks (e.g., [10], [13], [14]), with the latter aligning with our approach.

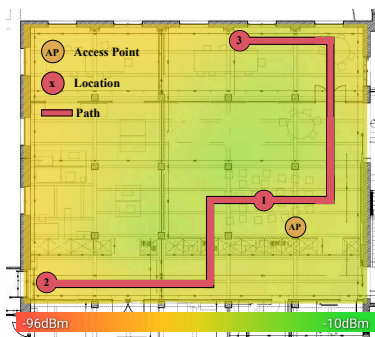


Fig. 11: CREW facilities floor plan, including a heatmap of RSSIs. Users begin at the central *Location 1* (near the AP), move together to *Location 2*, and return to *Location 1*. Then, both users move together to *Location 2* and return to *Location 1*. Finally, both users move to opposing locations (*User C* to *Location 2* and *User D* to *Location 3*) and return to *Location 1*.

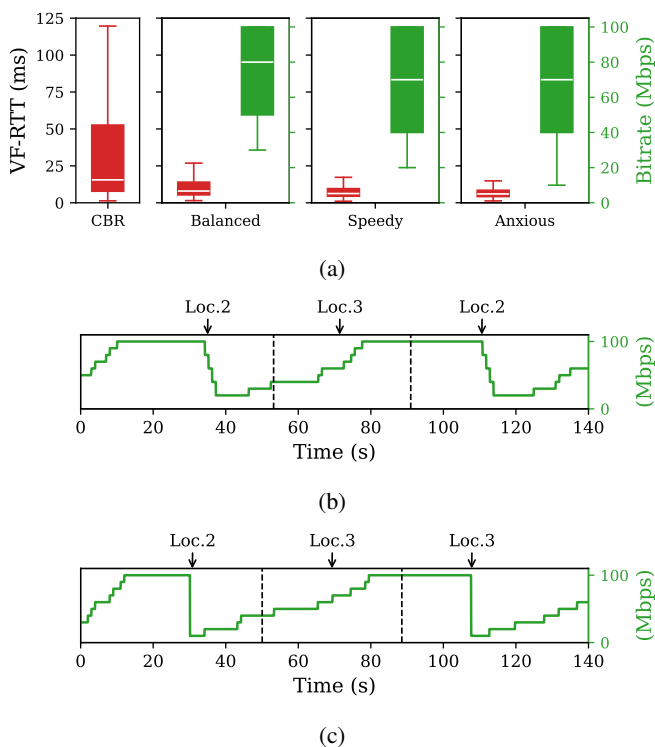


Fig. 12: Performance evaluation under multi-user mobility scenarios at CREW’s facilities: (a) VF-RTT and target bitrate distributions for *User C*, using CBR and NeSt-VR’s *Balanced*, *Speedy*, and *Anxious* profiles; (b) Target bitrate evolution using the *Speedy* profile (*User C*); (c) Target bitrate evolution using the *Anxious* profile (*User D*).

For instance, EveREst [13], [14], a VR-tailored ABR algorithm, estimates network bandwidth by measuring the throughput of lightweight frames and uses this estimate as an upper bound for bitrate selection, adjusting for the estimated number of concurrent users on the network. Despite EveREst, research on VR-specific ABR algorithms remains limited. [28] presents a fuzzy logic-based algorithm that adjusts bitrate according

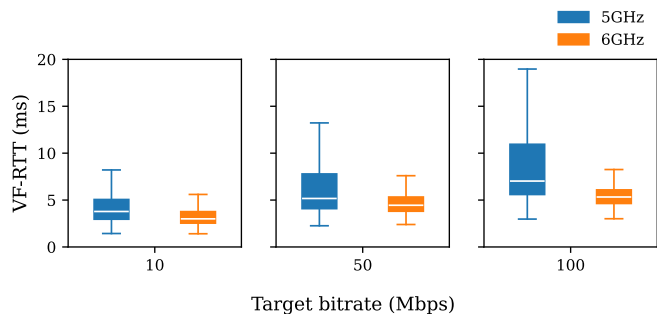


Fig. 13: VR streaming VF-RTT distributions for a single user in the 5 GHz and 6 GHz bands, with 10 Mbps, 50 Mbps, and 100 Mbps CBR.

to the server’s transmission buffer status, optimizing TCP transport for VR. [29] applies a delay-based congestion control mechanism inspired by Google’s WebRTC congestion control algorithm [12], which dynamically adjusts bitrate during video transmission based on one-way delay gradients. This ABR implementation is integrated into ALVR—which exhibits similar traffic patterns to WebRTC, where each VF is also sent in a single burst [30], [31]—and is evaluated in terms of motion-to-photon latency, user perception, and visual quality—measured using the Structural Similarity Measure (SSIM) and Peak Signal-to-Noise Ratio (PSNR). Similarly, [32] leverages ALVR and introduces a QoE-driven adaptation algorithm that dynamically adjusts encoding settings—including frame rate, resolution, and bitrate—based on real-time streaming metrics—such as throughput, packet loss, frame loss, and network delay—to maximize user QoE in cloud-based VR gaming scenarios. Other works also optimize parameters beyond bitrate. For instance, [33] proposes a deep reinforcement learning policy for 5G-based VR streaming that adjusts both network parameters (e.g., the number of allocated resource blocks) and application parameters (e.g., receiver buffer size, resolution) using streaming metrics—such as client frame rate, frame loss, and network delay—as well as network data—such as MCS and SNR—to optimize QoS and visual quality indicators like PSNR.

NeSt-VR strikes a balance between efficiency (selecting the highest feasible bitrate to maximize user experience) and stability (avoiding unnecessary bitrate fluctuations). Fairness in bandwidth allocation, typically evaluated using Jain’s fairness index [34] (a measure of the relative bandwidth distribution across multiple users) as demonstrated in [28] and [10], is partially addressed in NeSt-VR. NeSt-VR incorporates randomness into its gradual bitrate adjustments, preventing certain users from consistently consuming more bandwidth and thereby promoting a more equitable distribution of resources, while maintaining an acceptable QoS for all users. Other studies account for the potential presence and arrival of additional users in their bitrate adjustments, estimating how many VR streams the network can support based on its estimated capacity (e.g., [13], [14]) However, it may occur that not all users reduce their bitrate proportionally during periods of congestion. Addressing this would require cross-layer coord-

dination between users' ABRs [10] (e.g., [35]), enabling direct communication for managing bandwidth distribution, albeit at the cost of additional network overhead.

Traditional ABR algorithms for video streaming also incorporate QoE estimation to aid in bitrate decisions, often using objective video quality metrics such as PSNR, SSIM, or Video Multimethod Assessment Fusion (VMAF) scores [36] (e.g., [37], [38], [39]). Some other works incorporate QoE models. However, a standardized QoE function is not yet widely agreed upon, but many QoE-driven ABR solutions use variations of the Yin QoE objective function [40] (e.g., [32], [41], [42]). On the other hand, NeSt-VR's decision-making thresholds can be fine-tuned to ensure a satisfactory user experience without relying on traditional QoE metrics, as demonstrated in Tbl. VIII. Indeed, NeSt-VR leverages QoS-based network metrics—such as NFR and VF-RTT—as indicators of QoE, balancing video quality, smoothness, and latency in response to dynamic network conditions. NeSt-VR effectively reduces motion-to-photon latency and minimizes packet loss—two of the most critical QoE factors in VR streaming [9]—while preventing stalling, a major cause of cybersickness [43], thereby ensuring a consistent, immersive user experience.

B. Wi-Fi evolution and VR streaming

Wi-Fi 6, based on IEEE 802.11ax [44], [45], is used in all scenarios to evaluate NeSt-VR. Following [20], we configured Wi-Fi APs and clients with default Enhanced Distributed Channel Access (EDCA), as DL OFDMA/MU-MIMO provides no noticeable benefits, while UL OFDMA/MU-MIMO may introduce disrupt tracking packets due to AP scheduling [46]. With Wi-Fi 7, VR streaming could benefit from Multi-Link Operation (MLO), enabling lower latency and greater user support [47]. However, in dense Wi-Fi environments, MLO may still suffer from contention, potentially worsening delays due to the 'performance anomaly' [48]. To address this, Wi-Fi research and standardization efforts are exploring Multi-AP Coordination (MAPC) [4], which is expected to enhance transmission efficiency, resource allocation, and traffic prioritization across different Wi-Fi networks [49], improving latency and reliability for VR streaming [50]. The interplay of MLO, MAPC, and future Wi-Fi advancements with NeSt-VR remains an open question. While NeSt-VR is technology agnostic, incorporating awareness of Wi-Fi capabilities could further enhance its operation and performance.

IX. CONCLUSIONS

In this work, we have designed and implemented NeSt-VR, an ABR algorithm that dynamically adjusts bitrate based on network performance. Specifically, NeSt-VR lowers the bitrate during Wi-Fi congestion intervals—characterized by unsuccessful VF deliveries or prolonged delivery times—effectively mitigating packet loss and latency spikes while preserving video quality. It delivers enhanced performance in single-user, multi-user, and OBSS scenarios, both in lab and real-world environments. NeSt-VR leverages a set of newly introduced VR-specific performance metrics that offer critical

insights into network state and performance, supporting bitrate adaptation algorithms in their decision-making process.

To encourage further research on ABR algorithms for interactive VR streaming over Wi-Fi, we have made NeSt-VR and the VR performance metrics developed in this work publicly available on GitHub. We invite the community to build upon our work, whether by extending NeSt-VR or exploring entirely new solutions using it as a benchmark.

X. ACKNOWLEDGMENT

This work is partially funded by MAX-R (101070072) EU, Wi-XR PID2021-123995NB-I00 (MCIU/AEI/FEDER,UE), and by MCIN/AEI under the Maria de Maeztu Units of Excellence Programme (CEX2021-001195-M).

REFERENCES

- [1] Georgios Minopoulos and Konstantinos E Psannis. Opportunities and challenges of tangible XR applications for 5G networks and beyond. *IEEE Consumer Electronics Magazine*, 12(6):9–19, 2022.
- [2] Shu Shi and Cheng-Hsin Hsu. A survey of interactive remote rendering systems. *ACM Computing Surveys (CSUR)*, 47(4):1–29, 2015.
- [3] Ian F Akyildiz and Hongzhi Guo. Wireless extended reality (XR): Challenges and new research directions. *ITU J. Future Evol. Technol.*, 3(2):1–15, 2022.
- [4] Lorenzo Galati-Giordano, Giovanni Geraci, Marc Carrascosa, and Boris Bellalta. What will Wi-Fi 8 be? A primer on IEEE 802.11 bn ultra high reliability. *IEEE Communications Magazine*, 62(8):126–132, 2024.
- [5] Toni Adame, Marc Carrascosa-Zamacois, and Boris Bellalta. Time-sensitive networking in IEEE 802.11 be: On the way to low-latency WiFi 7. *Sensors*, 21(15):4954, 2021.
- [6] Lara Deek, Eduard Garcia-Villegas, Elizabeth Belding, Sung-Ju Lee, and Kevin Almeroth. Intelligent channel bonding in 802.11n WLANs. *IEEE Transactions on Mobile Computing*, 13(6):1242–1255, 2013.
- [7] Toni Adame, Marc Carrascosa, and Boris Bellalta. The TMB path loss model for 5 GHz indoor WiFi scenarios: On the empirical relationship between RSSI, MCS, and spatial streams. In *2019 Wireless Days (WD)*, pages 1–8. IEEE, 2019.
- [8] Sergio Barrachina-Muñoz, Boris Bellalta, and Edward W Knightly. Wi-Fi channel bonding: An all-channel system and experimental study from urban hotspots to a sold-out stadium. *IEEE/ACM Transactions on Networking*, 29(5):2101–2114, 2021.
- [9] Telecommunication Standardization Sector of ITU (ITU-T). Influencing factors on quality of experience for virtual reality services. ITU-T Recommendation G.1035, International Telecommunication Union (ITU), 2021.
- [10] Junchen Jiang, Vyas Sekar, and Hui Zhang. Improving fairness, efficiency, and stability in http-based adaptive video streaming with festive. In *Proceedings of the 8th international conference on Emerging networking experiments and technologies*, pages 97–108, 2012.
- [11] Kevin Spiteri, Rahul Uргаonkar, and Ramesh K. Sitaraman. BOLA: Near-Optimal Bitrate Adaptation for Online Videos. *IEEE/ACM Transactions on Networking*, 28(4):1698–1711, 2020.
- [12] Gaetano Carlucci, Luca De Cicco, Stefan Holmer, and Saverio Mascolo. Analysis and design of the google congestion control for web real-time communication (WebRTC). In *Proceedings of the 7th International Conference on Multimedia Systems, MMSys '16*, New York, NY, USA, 2016. Association for Computing Machinery.
- [13] Liubogoshchev, Mikhail and Korneev, Evgeny and Khorov, Evgeny. Everest: Bitrate adaptation for cloud vr. *Electronics*, 10(6):678, 2021.
- [14] Eugene Korneev, Mikhail Liubogoshchev, Dmitry Bankov, and Evgeny Khorov. How to Model Cloud VR: An Empirical Study of Features That Matter. *IEEE Open Journal of the Communications Society*, 2024.
- [15] Ferran Maura, Miguel Casasnovas, and Boris Bellalta. Experimenting with Adaptive Bitrate Algorithms for Virtual Reality Streaming over Wi-Fi. In *Proceedings of the 30th Annual International Conference on Mobile Computing and Networking*, pages 1930–1937, 2024.
- [16] Henning Schulzrinne, Stephen L. Casner, Ron Frederick, and Van Jacobson. RTP: A Transport Protocol for Real-Time Applications. RFC 3550, July 2003.

- [17] Telecommunication Standardization Sector of ITU (ITU-T). Quality of service assurance-related requirements and framework for virtual reality delivery using mobile edge computing supported by IMT-2020. ITU-T Recommendation Y.3109, International Telecommunication Union (ITU), 2021.
- [18] Telecommunication Standardization Sector of ITU (ITU-T). Functional requirements of E2E network platforms to enhance the delivery of cloud-VR services over integrated broadband cable networks. ITU-T Recommendation J.1631, International Telecommunication Union (ITU), 2021.
- [19] Martin Heusse, Franck Rousseau, Gilles Berger-Sabbatel, and Andrzej Duda. Performance anomaly of 802.11b. In *IEEE INFOCOM 2003. Twenty-second Annual Joint Conference of the IEEE Computer and Communications Societies (IEEE Cat. No. 03CH37428)*, volume 2, pages 836–843. IEEE, 2003.
- [20] Costas Michaelides, Miguel Casanovas, David Nunez, and Boris Bellalta. Lessons Learned From a Large-Scale Virtual Reality Experience Over Wi-Fi. *TechRxiv*, 2025.
- [21] Jetmir Haxhibeqiri, Xianjun Jiao, Xiaoman Shen, Chun Pan, Xingfeng Jiang, Jeroen Hoebeke, and Ingrid Moerman. Coordinated spatial reuse for wifi networks: A centralized approach. In *2024 IEEE 20th International Conference on Factory Communication Systems (WFCS)*, pages 1–8. IEEE, 2024.
- [22] Zhenzhe Zhong, Parag Kulkarni, Fengming Cao, Zhong Fan, and Simon Armour. Issues and challenges in dense wifi networks. In *2015 International Wireless Communications and Mobile Computing Conference (IWCMC)*, pages 947–951. IEEE, 2015.
- [23] Yusuf Sani, Andreas Mauthe, and Christopher Edwards. Adaptive Bitrate Selection: A Survey. *IEEE Communications Surveys & Tutorials*, 19(4):2985–3014, 2017.
- [24] Te-Yuan Huang, Ramesh Johari, Nick McKeown, Matthew Trunnell, and Mark Watson. A buffer-based approach to rate adaptation: evidence from a large video streaming service. *SIGCOMM Comput. Commun. Rev.*, 44(4):187–198, aug 2014.
- [25] James Curtis and Tony McGregor. Review of bandwidth estimation techniques. In *Proceedings of the New Zealand Computer Science Research Students' Conference*, volume 8, 2001.
- [26] Yoshua Bengio, Ian Goodfellow, and Aaron Courville. *Deep learning*, volume 1. MIT press Cambridge, MA, USA, 2017.
- [27] Aashish Gottipati, Sami Khairy, Gabriel Mittag, Vishak Gopal, and Ross Cutler. Offline to online learning for real-time bandwidth estimation, 2024.
- [28] Dimitrios J Vergados, Angelos Michalakis, Alexandros-Apostolos A Boulogeorgos, Spyridon Nikolaou, Nikolaos Asimopoulos, and Dimitrios D Vergados. Adaptive Virtual Reality Streaming: A Case for TCP. *IEEE Transactions on Network and Service Management*, 2023.
- [29] Ahmad Alhilar, Ze Wu, Yuk Hang Tsui, and Pan Hui. FovOptix: Human Vision-Compatible Video Encoding and Adaptive Streaming in VR Cloud Gaming. In *Proceedings of the 15th ACM Multimedia Systems Conference*, pages 67–77, 2024.
- [30] Marc Carrascosa and Boris Bellalta. Cloud-gaming: Analysis of google stadia traffic. *Computer Communications*, 188:99–116, 2022.
- [31] Miguel Casanovas, Costas Michaelides, Marc Carrascosa-Zamacois, and Boris Bellalta. Experimental Evaluation of Interactive Edge/Cloud Virtual Reality Gaming over Wi-Fi using Unity Render Streaming. *Computer Communications*, 2024.
- [32] Kuan-Yu Lee, Ashutosh Singla, Pablo Cesar, and Cheng-Hsin Hsu. Adaptive Cloud VR Gaming Optimized by Gamer QoE Models. *ACM Transactions on Multimedia Computing, Communications and Applications*, 2024.
- [33] Yaohua Sun, Jianmin Chen, Zeyu Wang, Mugen Peng, and Shiwen Mao. Enabling Mobile Virtual Reality with Open 5G, Fog Computing and Reinforcement Learning. *IEEE Network*, 36(6):142–149, 2022.
- [34] Rajendra K Jain, Dah-Ming W Chiu, William R Hawe, et al. A quantitative measure of fairness and discrimination. *Eastern Research Laboratory, Digital Equipment Corporation, Hudson, MA*, 21:1, 1984.
- [35] Xi Liu, Florin Dobrian, Henry Milner, Junchen Jiang, Vyas Sekar, Ion Stoica, and Hui Zhang. A case for a coordinated internet video control plane. In *Proceedings of the ACM SIGCOMM 2012 conference on Applications, technologies, architectures, and protocols for computer communication*, pages 359–370, 2012.
- [36] Reza Rassool. Vmaf reproducibility: Validating a perceptual practical video quality metric. In *2017 IEEE international symposium on broadband multimedia systems and broadcasting (BMSB)*, pages 1–2. IEEE, 2017.
- [37] Minsu Kim and Kwangsue Chung. HTTP adaptive streaming scheme based on reinforcement learning with edge computing assistance. *Journal of Network and Computer Applications*, 213:103604, 2023.
- [38] Hwanwook Lee, Yunmin Go, and Hwangjun Song. SDN-assisted HTTP adaptive streaming over Wi-Fi network. In *2018 Fifth International Conference on Software Defined Systems (SDS)*, pages 205–210. IEEE, 2018.
- [39] Siqi Huang and Jiang Xie. Dave: Dynamic adaptive video encoding for real-time video streaming applications. In *2021 18th Annual IEEE International Conference on Sensing, Communication, and Networking (SECON)*, pages 1–9, 2021.
- [40] Xiaoqi Yin, Abhishek Jindal, Vyas Sekar, and Bruno Sinopoli. A control-theoretic approach for dynamic adaptive video streaming over HTTP. In *Proceedings of the 2015 ACM Conference on Special Interest Group on Data Communication*, pages 325–338, 2015.
- [41] Wenjia Wu, Jiale Yuan, Sheng Ma, and Ming Yang. AP-assisted adaptive video streaming in wireless networks with high-density clients. *Computer Communications*, 219:53–63, 2024.
- [42] Zheng Chang, Xiang Zhou, Zhi Wang, Hanyang Li, and Xing Zhang. Edge-assisted adaptive video streaming with deep learning in mobile edge networks. In *2019 IEEE Wireless Communications and Networking Conference (WCNC)*, pages 1–6. IEEE, 2019.
- [43] Muhammad Shahid Anwar, Jing Wang, Sadique Ahmad, Asad Ullah, Wahab Khan, and Zesong Fei. Evaluating the factors affecting qoe of 360-degree videos and cybersickness levels predictions in virtual reality. *Electronics*, 9(9):1530, 2020.
- [44] Boris Bellalta. IEEE 802.11ax: High-efficiency WLANs. *IEEE wireless communications*, 23(1):38–46, 2016.
- [45] Evgeny Khorov, Anton Kiryanov, Andrey Lyakhov, and Giuseppe Bianchi. A tutorial on IEEE 802.11 ax high efficiency WLANs. *IEEE Communications Surveys & Tutorials*, 21(1):197–216, 2018.
- [46] Costas Michaelides, Miguel Casanovas, Daniele Marchitelli, and Boris Bellalta. Is Wi-Fi 6 Ready for Virtual Reality Mayhem? A Case Study Using One AP and Three HMDs. In *2023 IEEE Future Networks World Forum (FNWF)*, pages 1–6. IEEE, 2023.
- [47] Marc Carrascosa-Zamacois, Lorenzo Galati-Giordano, Francesc Wilhelm, Gianluca Fontanesi, Anders Jonsson, Giovanni Geraci, and Boris Bellalta. Performance Evaluation of MLO for XR Streaming: Can Wi-Fi 7 Meet the Expectations? *IEEE CAMAD 2024.*, 2024.
- [48] Marc Carrascosa-Zamacois, Giovanni Geraci, Lorenzo Galati-Giordano, Anders Jonsson, and Boris Bellalta. Understanding multi-link operation in Wi-Fi 7: Performance, anomalies, and solutions. In *2023 IEEE 34th Annual International Symposium on Personal, Indoor and Mobile Radio Communications (PIMRC)*, pages 1–6. IEEE, 2023.
- [49] David Nunez, Malcom Smith, and Boris Bellalta. Multi-AP coordinated spatial reuse for Wi-Fi 8: Group creation and scheduling. In *2023 21st Mediterranean Communication and Computer Networking Conference (MedComNet)*, pages 203–208. IEEE, 2023.
- [50] Kirill Chemrov, Dmitry Bankov, Evgeny Khorov, and Andrey Lyakhov. Support of Real-Time Applications in Wi-Fi 8 with Multi-Ap Coordinated Parameterized Spatial Reuse. In *2023 IEEE International Black Sea Conference on Communications and Networking (BlackSeaCom)*, pages 226–231. IEEE, 2023.